AUV-based acoustic observations of the distribution and patchiness of pelagic scattering layers during midnight sun

Authors: Maxime Geoffroy[1], Finlo R. Cottier[2,1], Jørgen Berge[1,3], Mark E. Inall[2,4]

[1] *UiT, The Arctic University of Norway, Faculty of Biosciences, Fisheries and Economics, Department of Arctic and Marine Biology, 9037 Tromsø, Norway*

[2] *Scottish Association for Marine Science, Scottish Marine Institute, Oban, Argyll PA37 1QA, United Kingdom*

[3] *University Centre in Svalbard, Pb 156, N-9171, Longyearbyen, Norway*

[4] *University of Edinburgh, Department of Geosciences, Grant Institute, Edinburgh, United Kingdom*

Corresponding author:

Maxime Geoffroy (maxime.geoffroy@uit.no)

Phone: +47 776 44447

Abstract

An Autonomous Underwater Vehicle (AUV) carrying 614 kHz RDI Acoustic Doppler Current Profilers (ADCPs) was deployed at four locations over the West Spitsbergen outer shelf in July 2010. The backscatter signal recorded by the ADCPs was extracted and analysed to investigate the vertical distribution and patchiness of pelagic organisms during midnight sun. At the northernmost locations (Norskebanken and Woodfjorden), fresher and colder water prevailed in the surface layer (0-20 m) and scatterers (interpreted as zooplankton and micronekton) were mainly distributed below the pycnocline. In contrast, more saline and warmer Atlantic Water dominated the surface layer at Kongsfjordbanken and Isfjordbanken and scatterers were concentrated in the top 20 m, above the pycnocline. Pelagic scatterers formed patchy aggregations at all locations, but patchiness generally increased with the density of organisms and decreased at depths >80 m. This study contributes to our understanding of the vertical distribution of pelagic organisms in the Arctic, and the spatial coverage of the AUV has extended early acoustic studies limited to Arctic fjords from 1-dimensional observations to a broader offshore coverage. Neither synchronised nor unsynchronized vertical migrations were detected, but autonomous vehicles with limited autonomy (<1 day) may not be as effective as long-term mooring deployments or long-range AUVs to study vertical migrations. Short-term AUV-based acoustic surveys of the pelagic communities are nonetheless highly complementary to Eulerian studies, in particular by providing spatial measurements of patchiness. Compared with ship-based or moored acoustic instruments, the 3D trajectory of AUVs also allows using acoustic instruments with higher frequencies and better size resolution, as well as the detection of organisms closer to the surface.

Keywords: AUV, ADCP, backscatter, zooplankton, micronekton, distribution, patchiness, vertical migrations, Spitsbergen, Arctic

Introduction

Fundamental aspects of the abundance, lifecycle, vertical distribution, and migratory behaviour of zooplankton and nekton in the Arctic have been studied using traditional net techniques (e.g. Falk-Petersen *et al.,* 2007; Eisner *et al*., 2013; Darnis and Fortier, 2014) and through the use of acoustics (e.g. La *et al*., 2015; Geoffroy *et al*., 2016). For instance, Acoustic Doppler Current Profilers (ADCPs) have been used to document the variations in behaviour of pelagic scatterers with temporal resolution ranging from minutes to seasons (Wallace *et al*., 2010; Last *et al*., 2016). The community composition of assemblages detected by acoustics has been estimated from net samples or sediment trap content (e.g. Cottier *et al*., 2006; Wallace *et al*., 2010; Berge *et al*., 2014). ADCPs are primarily deployed to measure current velocity, but their backscatter data can reveal detailed information about the pelagic ecosystem when multi-frequency scientific echosounders are not available (Brierley *et al*., 2006; Valle-Levinson *et al*., 2014). However,, most ADCP studies on the vertical distribution of pelagic scatterers in the Arctic have been based on Eulerian sampling and lack spatial resolution (e.g. Cottier *et al*., 2006; Berge *et al*., 2014; Last *et al*., 2016). Spatial patchiness remains particularly difficult to measure using data from nets or moored instruments.

Autonomous Underwater Vehicles (AUVs) represent an alternative to Eulerian platforms and allow spatial surveys of the water column (Fernandes *et al*., 2003; Schofield *et al*., 2010; Berge *et al*., 2012). AUVs have a longer operational range and are less vulnerable to bad weather than remotely operated vehicles. They access areas too shallow for scientific vessels (An *et al*., 2001), and can survey under an ice cover (Brierley *et al*., 2002). Acoustic devices mounted on AUVs can survey closer to the surface (Boyd *et al*., 2010) or seabed compared with moored or ship-mounted instruments, thus reducing the surface blind zone and bottom dead zone (i.e. blind areas respectively created by the near-field and the conical shape of the acoustic beam; Scalabrin *et al*., 2009). In addition, a 3D trajectory allows AUVs to approach targets close enough to use higher frequency acoustic instruments with better size resolution (Fernandes *et al*., 2003).

In July 2010, an AUV fitted with turbulence sensors, ADCPs, and a CTD was deployed at four locations to study the physical oceanographic environment over the West Spitsbergen outer shelf (Steele *et al*., 2012). Here, we analyse data from the downward- and upward-looking ADCPs to investigate vertical distributions and patchiness of pelagic scatterers over a larger geographical area than previous studies limited to an Arctic fjord (Cottier *et al*., 2006; Berge *et al*., 2014). Specifically, we aim to test the hypotheses that (1) vertical migrations are limited to unsynchronised behaviour during midnight sun (Cottier *et al*., 2006); and (2) hydrography determines the depth of pelagic organisms when they are not migrating (Berge *et al*., 2014). Advantages and limitations of using AUV-mounted ADCPs for biological studies are further discussed.

Material and methods

Study design and area

A Kongsberg Hydroid REMUS AUV, depth rated to 600 m, was deployed in the NW sector of Spitsbergen at four locations on five different occasions (Figure 1) between 6 and 20 July 2010 (Table 1). The oceanographic conditions in this region are dominated by the presence of relatively warm and saline Atlantic Water (AW: T >3.0°C, S >34.65), carried northward along the slope by the West Spitsbergen Current (Saloranta and Hogan, 2001; Cottier *et al*., 2005). On the shelf, and forming a front with the AW, is a seasonally varying presence of cooler and fresher Arctic Water (ArW: -1.5°C< T <1.0°C, 34.30< S <34.80) (Svendsen *et al*., 2002; Cottier and Venables, 2007).

For each deployment, AUV-based sampling consisted of four to seven horizontal transects, each of 5-10 km and conducted at depths ranging from 10 m to 170 m (Figure 2 a-e). The AUV surfaced at the completion of each transect to acquire a GPS position and to communicate with the AUV operators by WiFi or Iridium. In total, the survey covered an area of ~24 km^2 over the outer shelf (Figure 2 a-e; right column). The sun remained above the horizon throughout the study giving continuous (though not constant) illumination. Deployments at Norskebanken, Woodfjorden, and Kongsfjordbanken were conducted in the middle of the day, when the sun elevation was between 22 and 35°. The deployment at Isfjordbanken was conducted around midnight, when the sun elevation was between 13 and 15° (http://www.sunearthtools.com; accessed on 17 April 2016).

Acoustic and environmental data collection

The AUV recorded acoustic data, temperature, and salinity along transects (see Steele *et al*., 2012 for further details). Two RDI 614 kHz ADCPs mounted on the AUV, one looking upward and another downward, recorded the raw acoustic backscatter to about 42 m both above and below the vehicle. The AUV cruised at 3-4 knots and the ping rate of the ADCPs varied from 1 ping each 6 to 7.7 seconds, resulting in a horizontal resolution between 9 and 16 m.

A CTD mounted on the AUV recorded temperature-salinity profiles to calculate (1) speed of sound; (2) the coefficient of absorption; and (3) density gradient profiles used to determine the depth and water density at the pycnocline. In the analysis of backscatter data, we followed Cottier *et al*. (2006) and partitioned the water column into three layers: (1) the Surface Layer (SL; 0-20 m), an Intermediate Layer (IL; 20-80 m), and a Deeper Layer (DL; > 80 m).

Backscatter data

The acoustic volume backscattering strength (S_v in dB re 1 m^{-1}) is an indication of the density of scatterers in a given volume. Because the 614 kHz ADCP signal can detect single targets as small as ~2.4 mm (i.e. wavelength at c = 1500 $m \cdot s^{-1}$), most of the backscatter measured here can likely be attributed to meso- and macrozooplankton (Lorke *et al*., 2004). Although fish are better detected at higher frequencies, micronekton also likely contributed to a portion of the backscatter (e.g. Benoit-Bird, 2009).

S_v was calculated from raw data using the SONAR equation adapted for ADCPs (Deines, 1999). The coefficient of absorption (α) used to calculate the Time-Varied-Gain (TVG = $40\log_{10}R + 2\alpha R$, where R is the range from the transducer) was estimated from mean temperature and salinity values recorded with the AUV-mounted CTD. The inclusion of a maximum S_v threshold of -45 dB discarded potential stronger echoes from large targets and noise. A Time-Varied-Threshold (TVT = $20\log R + 2\alpha R - 142$), selected with an iteration process on echoes typical of noise, was added to offset noise amplification at depth by the TVG (e.g. Benoit *et al*., 2008; Geoffroy *et al*., 2016). Data from the upward looking ADCP in Kongsfjordbanken on 06 July were polluted by noise and removed from the analysis. For each ping, S_v values were calculated over 4 m vertical bins to be consistent with previous ADCP-based studies (Cottier *et al*., 2006; Wallace *et al*., 2010; Berge *et al*., 2014). For each deployment, linear s_v values from all bins of the same depth were averaged and associated with mean temperature and salinity at each depth.

Vertical velocity anomalies

To verify the occurrence of unsynchronized vertical migrations, vertical velocity anomalies (w') were calculated for each bin by subtracting the average vertical speed for the entire deployment from the vertical speed within that bin (Cottier *et al*., 2006). A positive mean w' for a given bin corresponds to an overall upward migration, while negative values indicate downward migrations. To limit biases from the vertical movement of the AUV, only vertical speed measurements collected at fixed depths were used for these calculations and aberrant values (>15 $mm \cdot s^{-1}$ or >4-fold mean speed) were discarded.

Estimation of density and calculation of the patchiness index

To calculate patchiness indices, we derived an estimate of the density of scatterers (ρ_v in $ind \cdot m^{-3}$) within each bin (1 ping horizontally × 4 m vertically):

$$\rho_v = \frac{s_v}{\sigma_{bs}} \tag{1}$$

s_v is the linear volume scattering strength ($m^2 \cdot m^{-3}$) and σ_{bs} the cross-sectional area of the average scatterer (Parker-Stetter *et al*., 2009).

No net samples were collected in the vicinity of the AUV deployments, but as the 614 kHz signal is likely dominated by zooplankton we estimated an average Target Strength (TS) of -89.94 dB re 1 m^2 based on the average zooplankton scatterer captured by Cottier *et al*. (2006) and using the randomly oriented fluid bent-cylinder model (Stanton *et al*., 1994). The corresponding σ_{bs} was 1×10^{-9} m^2 (equation 2):

$$\sigma_{bs} = 10^{\left(\mathrm{TS}/_{10}\right)} \tag{2}$$

For each deployment, the Lloyd's patchiness index *P* (Lloyd, 1967) within the SL, IL, and DL was then calculated using equation 3:

$$P = \left[\frac{\overline{\rho_v} + \left[\left(\frac{s^2}{\overline{\rho_v}}\right) - 1\right]}{\overline{\rho_v}}\right] \tag{3}$$

where $\overline{\rho_v}$ represents the mean density of individuals within a given layer and s^2 is the sample variance. *P* depends on the spatial distribution of scatterers and describes how many other individuals are in the sample relative to a random distribution. $P<1$ indicates a uniform distribution, $P=1$ corresponds to a random (i.e. Poisson) distribution, and $P>1$ indicates an aggregating behaviour. The index increases with increased patchiness. For instance, $P=2$ if individuals are twice as crowded compared to a random distribution (Lloyd, 1967; Houde and Lovdal, 1985; De Robertis, 2002). The spatial scale of patchiness measurements corresponds to the sampling scale, in our case 9-16 m horizontally (i.e. one ping) by 4 m vertically.

Results

Water masses and vertical distribution of pelagic scatterers

At the northern sites (Norskebanken and Woodfjorden), salinity and temperature in the SL were lower (S <34.58, T <5.07 °C; Figure 3 a-b) than at the southernmost locations (Kongsfjordbanken and Isfjordbanken), indicating less influence of AW. Backscatter values higher than the mean s_v for the entire deployment were concentrated within the first four metres and below the 1027.84 and 1027.63 kg·m^{-3} isopycnal lines, respectively (Figure 4 a-b; left panels). These water densities coincide with a stabilisation in the density gradient profiles, and thus roughly correspond to the base of the pycnocline (BOP; Figure 4 a-b; right panels). In contrast, surface water (0-20 m) at Kongsfjordbanken and Isfjodbanken was more saline and warmer (S<35.20, T<6.60 °C; Figure 3 a-b) than at the northernmost locations, and backscatter values higher than average were concentrated above the 1027.7 and 1027.8 kg·m^{-3} isopycnal lines (Figure 4 c-e; left panels), which also roughly correspond to the BOP (Figure 4 c-e; right panels).

No isolated dense echoes typical of fish schools were detected, supporting the idea that the pelagic scattering layers were mainly composed of zooplankton. The backscatter at Norskebanken remained low (<85 dB) from the surface to the maximum sampling depth of 150 m (Figure 5a), indicating low densities of scatterers. At Woodfjorden, the backscatter reached maximal values at the surface, decreased down to 40 m, increased until 70 m, and decreased at greater depths (Figure 5b). At the southernmost locations (Konsfjordbanken and Isfjordbanken), S_v values were significantly higher in the SL than in the IL and DL (Tuckey HSD; $p<0.001$) (Figure 5 c-e). Maximal backscatter occurred near the surface and decreased linearly with depth until 80 m (S_v = -0.2×Depth-78.3; r^2=0.73; $p<1\times10^{-15}$; n=60) (Figure 5 f).

The vertical distribution of the backscatter was similar at both southernmost locations, despite the fact that data were collected during midday at Kongsfjordbanken and around midnight at Isfjordbanken. Mean linear backscatter did not differ significantly within the SL (Kruskal-Wallis; p=0.54) or the DL (Kruskal-Wallis; p=0.63), although the median was slightly higher in the SL at midnight (Figure 6 a and c). In the IL, mean backscatter was similar between the first deployment at Kongsfjordbanken (06 July) and the deployment at Isfjordbanken, but was significantly higher at Kongsfjordbanken on 12 July (Kruskal-Wallis; p=0.007; Figure 6b). However, the backscatter variance was high for all deployments (Figure 6 a-c).

Positive and negative vertical velocity anomaly values (w') were measured at all depths and all locations (Figure7 a-e; left column). Upward movement (positive w' values) of scatterers were mainly measured above 80 m at Norskebanken, 40 m at Woodfjorden, and 90 m at Isfjordbanken, while downward migrations (negative w' values) were measured deeper (Figure 7 a, b, e; right column). The direction was inverted at Kongsfjordbanken, with downward migrations above 80 m (06 July 06) or 40 m (12 July) and upward movement at greater depths (Figure 7 c, d; right column). Although time-averaged w' measured within each 4 m changed between the surface layers and at depth, suggesting different migration directions, variance was high (typically ±2 mm s^{-1}) and average w' values were low (typically much less than ± 1 $mm \cdot s^{-1}$) at all locations (Figure 7; right column).

Density and patchiness

The estimated mean density of scatterers at the northernmost locations was more uniform with depth compared to the southernmost sites (Figure 8; left panel). The estimated density remained between 0.9 and 1.0 $ind \cdot m^{-3}$ at Norskebanken (Figure 8a; left panel), and between 2.4 and 4.0 $ind \cdot m^{-3}$ at Woodfjorden (Figure 8b; left panel). At Kongsfjordbanken and Isfjordbanken, the estimated density varied from 9.1 to 13.6 $ind \cdot m^{-3}$ in the SL, from 2.2 to 6.3 $ind \cdot m^{-3}$ in the IL, and from 0.6 to 0.8 $ind \cdot m^{-3}$ at greater depths (Figure 8 c-e; left panels). Lloyd's index of patchiness (P) was >1 in the SL at all locations, indicating patchy distributions near the surface (Figure 8 a-e; right panel). Distributions were generally less patchy in the IL, and at Norskebanken the distribution was uniform in the IL (P<1: Figure 8a; right panel). In contrast, at Kongsfjordbanken the patchiness increased in the IL compared to the SL (Figure 8 c-d; right panels). Compared to the SL, patchiness in the DL decreased at all locations with uniform distributions at Norskebanken and Isfjordbanken (Figure 8 a and e; right panels). The patchiness index was over one order of magnitude higher in the SL at Norskebanken and Woodfjorden than anywhere else, indicating ten times patchier distributions (Figure 8 a-b; right panels). Apart from these two observations, patchiness was significantly correlated with the density of scatterers (Spearman rank correlation; ρ=0.56; p=0.016) (Figure 9).

Discussion

The 3D trajectory of the AUV allowed documenting the 614 kHz backscatter from <1.5 m below the surface to vertical ranges up to 200 m (Figure 2). In comparison, the surface blind zone of ship-based surveys reaches ~15 m (Scalabrin et al., 2009), and if a similar ADCP had been installed on a mooring at depth the vertical range would not have been greater than 40 m. The extended vertical and spatial ranges conferred by the 3D trajectory of the AUV allowed obtaining valuable insights into synchronised and unsynchronised vertical migrations during midnight sun, documenting the vertical distribution of pelagic scatterers in relation to hydrography, and demonstrating that their patchiness increased with the density of organisms.

Synchronised and unsynchronised vertical migrations during midnight sun

The vertical distributions of backscatter during midday and around midnight at the two southernmost locations were statistically similar (Figure 5) and interpreted as an absence of synchronised Diel Vertical Migration (DVM), as generally reported during periods of continuous illumination in the Arctic (Fischer and Visbeck, 1993; Blachowiak-Samolyk *et al*., 2006; Cottier *et al*., 2006). While synchronised DVM does not generally occur during continuous illumination at high latitudes, an alternate behaviour of unsynchronized vertical migration, with animals migrating independently of each other in response to their individual needs, has been reported from May to July in Arctic fjord environments (Cottier *et al*., 2006; Wallace *et al*., 2010). These migrations occur continuously during a 24-hour period and do not modify the total abundance of scatterers within each layer. However, unsynchronized migrations can be identified in ADCP records when the mean direction of migration in the SL is downward (indicated by negative w' values) and the mean direction of migration in the IL and DL is upward (indicated by positive w' values; details in Cottier *et al*., 2006). In this study, mean values of w' were positive (upward) in the SL and negative (downward) in the DL at most locations, except for Kongsfjordbanken where the opposite occurred. Even at Kongsfjordbanken, variance was high and w' measurements were low compared to previous studies that have documented unsynchronized migrations (e.g. -8 to 8 $mm \cdot s^{-1}$; Cottier *et al*., 2006). In contrast to previous observations in Arctic fjords, our data thus suggest that pelagic scatterers do not perform clear unsynchronized migrations over the outer shelf during midnight sun. Accordingly, their contribution to the biological pump is likely reduced at that time of the year (Tarling and Johnson, 2006; Wallace *et al*., 2013).

It is important to note that the period of averaging w' during this study (less than 7 hours) was less than 5% that of Cottier *et al*. (2006) and Wallace *et al*. (2013) (7 days). Given the high variance in w', the detection of unsynchronized migratory behaviours of planktonic organisms may require longer duration surveys. Furthermore, as most AUVs cannot cover 24-hour cycles, the detection of DVM in the Arctic using this technique is limited to comparisons between midday and midnight surveys. Hence, even though our results suggest an absence of unsynchronised and synchronised vertical migrations in the outer shelf environment during midnight sun, such migrations could possibly occur. Long-range AUVs (e.g. Hobson *et al*., 2012) were recently developed and they could overcome this issue by combining the benefits of AUVs to that of multi-day deployments on Eulerian platforms.

Vertical distribution of pelagic scatterers in relation to hydrography

Although the vertical distributions of pelagic organisms, in particular zooplankton, are mainly related to changes in light intensity, Berge *et al*. (2014) suggested that hydrographic structures can determine resting depth of zooplankton between migration events. As no vertical migrations were detected during this study, it is likely that other factors, including hydrography, influenced the vertical distribution of scatterers.

With the exception of a few patchy aggregations in the top 4 m, scatterers at the northernmost locations were distributed below the pycnocline, as previously documented for Arctic fjords (Berge *et al*., 2014) and during laboratory experiments (Lougee *et al*., 2002). These small pelagic organisms likely avoided colder and fresher surface waters to remain in denser and deeper water masses, where higher viscosities require less energy to hold position (Harder, 1968) and temperatures are closer to thermal preferences (Berge *et al*., 2014). In contrast, density and temperature were higher at the southernmost locations so scatterers remained within and above the pycnocline. We surmise that discrepancies in vertical distributions of the pelagic scattering layers between the northernmost and southernmost locations derived in part from different hydrographic regimes, in addition to other factors such as variations in the zooplankton assemblages and in primary production (Blachowiak-Samolyk *et al*., 2008). Furthermore, this study supports the idea that the pycnocline acts as a physical barrier limiting vertical migrations of small pelagic organisms and contributing to their retention in either the SL or at depth (Lougee *et al*., 2002). Therefore, in addition to continuous solar irradiance, the strong density gradient prevailing during Arctic summer may contribute to the absence of vertical migrations between different water masses.

Increased patchiness with density

Due to increased spatial range, AUV-mounted ADCPs provide better spatial resolution of patchiness than moored ADCPs (e.g. Brierley *et al*., 2006) or multi-net samplers (e.g. Vogedes *et al*., 2014). Our results are nonetheless consistent with previous observations of an aggregating behaviour for *Calanus* spp. in Isfjorden in July (Vogedes *et al*., 2014). However, our mean density estimates remained below 14 ind·m^{-3}, while previous plankton net-based studies conducted in fjords reported zooplankton densities from 76 to >200 ind·m^{-3} in the first hundred metres of the water column (Kwasniewski *et al*., 2003; Cottier *et al*., 2006; Berge *et al*., 2014). These results suggest considerably lower abundances of pelagic scatterers over the outer shelf than within fjords, supporting previous work by Daase and Eiane (2007) in northern Spitsbergen. If patchiness increases with density (Figure 9), then patchy aggregations are expected to be more abundant in fjords compared with outer shelf locations.

Lloyd (1967) developed the patchiness index P (equation 4) to study the “mean crowding” of animals or plants. In the marine environment, the index proved useful to document the patchiness of fish eggs and ichthyoplankton (e.g. McQuinn *et al*., 1983; Houde and Lovdal, 1985; Maynou *et al*., 2006) and zooplankton (e.g. George, 1981; De Robertis, 2002; Greer *et al*., 2013). Bez (2000) indicated that the Lloyd’s patchiness index is biased when calculated from densities rather than counts, as in the present study.

Nonetheless, by comparing the index calculated from zooplankton backscatter data (density) with *P* computed from the total number of targets in a simulated acoustic image (counts), De Robertis (2002) demonstrated that, despite sampling biases resulting in conservative values, *P* can efficiently be used as a measure of aggregation at low target densities, such as those observed here. Biases could also originate from the average cross section of scatterers used for calculations, which was based on the average copepod cross section at Kongsfjorden (Cottier *et al*., 2006). The mean cross section (σ_{bs}) of scatterers could have been different offshore, which would have biased density and patchiness calculations. The patchiness index calculated here nonetheless provides a relative measure between vertical layers (SL, IL and DL) and acts as a baseline indicator for the patchiness of pelagic organisms in the Arctic.

The scatterers exhibited a strong aggregating behaviour, most likely to dilute predation risk by visual predators, maximise food capture, and optimise energy expenditure (Folt and Burns, 1999; Ritz, 2000). The very high patchiness indices in the SL at Norskebanken and Woodfjorden resulted from a generally low density with few dense and small aggregations just below the surface (Figure 2 a-b; left column), although patchiness generally increased with scatterer density. Patchiness may also partly explain the significantly higher backscatter in the IL at Kongsfjordbanken on 12 July compared to 06 July (Figure 6b), as a non-uniform distribution is likely to result in variations among deployments. Another possible explanation for variations in density and patchiness in the IL between deployments at Kongsfjordbanken might be the paucity of samples at certain depths on 06 July. Some sections of the water column were then only surveyed during ascent or descent of the AUV and patches of zooplankton or micronekton could have been missed (Figure 2 c-d). At small scales (metres), physical turbulence can also determine the spatial distribution of pelagic organisms and facilitates the formation of aggregations (Mackas *et al*., 1997; De Robertis, 2002). During the survey, turbulence was higher in the SL and decreased with depth (Steele *et al*., 2012). Because patchiness followed a similar trend, it is possible that it was correlated with turbulence, in addition to the density of scatterers.

Conclusions

The use of an AUV allowed investigating key aspects of the distribution and behaviour of Arctic pelagic organisms over larger spatial scales than previously reported. The AUV also enabled measurements of additional spatial variables, such as patchiness indices. This study supports the hypothesis that, in the absence of vertical migration, hydrographic structures influence vertical distributions of pelagic organisms on a regional scale. In particular, the pycnocline could represent a physical barrier that retains organisms in either the surface layer or below the strongest density gradient. Scatterers consistently formed patchy aggregations in the top 20 m, which stresses both the ecological importance of this layer for predators and the need for prudent interpretations when calculating abundances from stationary net deployments. AUV-based acoustic surveys of the pelagic communities are complementary to Eulerian studies, for instance by providing spatial measurements of patchiness. The 3D trajectory of AUVs allows approaching targets sufficiently close to use high frequency acoustic instruments with high size resolution and, by reducing the surface blind zone to <1.5 m, enables detection of aggregations close to the surface. However, future surveys of vertical migrations by planktonic organisms would benefit from the deployment of long-range AUVs to cover several daily cycles.

Acknowledgements

This work results from an internship financially supported by Québec-Océan at Université Laval, Canada, and hosted by the Scottish Association for Marine Science. We thank the Master and crew of the RSS James Clark Ross and the scientists and technical support staff of Cruise JR219, in particular Tim Boyd, Colin Griffiths and Estelle Dumont for AUV deployments. Field work was funded by the UK Natural Environment Research Council (under the Oceans 2025 programme and National Capability support for the Scottish Marine Robotics Facility). We are also grateful to Matt Toberman and Laura Hobbs for advice while developing the data processing algorithm, and to Gérald Darnis for reviewing the manuscript. This study is a contribution to the Norges Forskningsråd project *Arctic ABC* number 244319.

References

An, E., Dhanak, M. R., Shay, L. K., Smith, S., and Van Leer, J. 2001. Coastal oceanography using a small AUV. Journal of Atmospheric and Oceanic Technology, 18: 215-234.

Benoit, D., Simard, Y., and Fortier, L. 2008. Hydroacoustic detection of large winter aggregations of Arctic cod (*Boreogadus saida*) at depth in ice-covered Franklin Bay (Beaufort Sea). Journal of Geophysical Research: Oceans,113: C6.

Benoit-Bird, K. J. 2009. The effects of scattering-layer composition, animal size, and numerical density on the frequency response of volume backscatter. ICES Journal of Marine Science, 66: 582-593.

Berge, J., Batnes, A. S., Johnsen, G., Blackwell, S. M., and Moline, M. A. 2012. Bioluminescence in the high Arctic during the polar night. Marine Biology, 159: 231-237.

Berge, J., Cottier, F., Varpe, Ø., Renaud, P. E., Falk-Petersen, S., Kwasniewski, S., Griffiths, C., *et al*. 2014. Arctic complexity: a case study on diel vertical migration of zooplankton. Journal of Plankton Research, 36: 1279-1297.

Bez, N. 2000. On the use of Lloyd's index of patchiness. Fisheries Oceanography, 9: 372-376.

Blachowiak-Samolyk, K., Søreide, J. E., Kwasniewski, S., Sundfjord, A., Hop, H., Falk-Petersen, S., and Hegseth, E. N. 2008. Hydrodynamic control of mesozooplankton abundance and biomass in northern Svalbard waters (79-81 degrees N). Deep-Sea Research Part II, 55: 2210-2224.

Blachowiak-Samolyk, K., Kwasniewski, S., Richardson, K., Dmoch, K., Hansen, E., Hop, H., Falk-Petersen, S., and Mouritsen, L.T. 2006. Arctic zooplankton do not perform diel vertical migration (DVM) during periods of midnight sun. Marine Ecology Progress Series, 308: 101-116.

Boyd, T., Inall, M., Dumont, E., and Griffiths, C. 2010. AUV observations of mixing in the tidal outflow from a Scottish sea loch. *In* Autonomous Underwater Vehicles (AUV), pp. 1-9. IEEE.

Brierley, A. S., Fernandes, P. G., Brandon, M. A., Armstrong, F., Millard, N. W., McPhail, S. D., Stevenson, P., *et al*. 2002. Antarctic krill under sea ice: Elevated abundance in a narrow band just south of ice edge. Science, 295: 1890-1892.

Brierley, A. S., Saunders, R. A., Bone, D. G., Murphy, E. J., Enderlein, P., Conti, S. G., and Demer, D. A. 2006. Use of moored acoustic instruments to measure short-term variability in abundance of Antarctic krill. Limnology and Oceanography Methods, 4: 18-29.

Cottier, F. R., Tarling, G. A.,Wold, A., and Falk-Petersen, S. 2006. Unsynchronized and synchronised vertical migration of zooplankton in a high Arctic fjord. Limnology and Oceanography, 51: 2586-2599.

Cottier, F. R., Tverberg, V., Inall, M., Svendsen, H., Nilsen, F., and Griffiths, C. 2005. Water mass modification in an Arctic fjord through cross-shelf exchange: The seasonal hydrography of Kongsfjorden, Svalbard. Journal of Geophysical Research: Oceans, 110: C12005.

Cottier, F. R., and Venables, E. J. 2007. On the double-diffusive and cabbeling environment of the Arctic Front, West Spitsbergen. Polar Research, 26: 152–159.

Daase, M., and Eiane, K. 2007. Mesozooplankton distribution in northern Svalbard waters in relation to hydrography. Polar Biology, 30: 969-81.

Darnis, G., and Fortier, L. 2014. Temperature, food and the seasonal vertical migration of key Arctic copepods in the thermally stratified Amundsen Gulf (Beaufort Sea, Arctic Ocean). Journal of Plankton Research, 36: 1092-1108.

Deines, K. L. 1999. Backscatter estimation using broadband acoustic Doppler current profilers. *In* Current measurement, pp. 249-253. IEEE.

De Robertis, A. 2002. Small-scale spatial distribution of the euphausiid *Euphausia pacifica* and overlap with planktivorous fishes. Journal of Plankton Research, 24: 1207-1220.

Eisner, L., Hillgruber, N., Martinson, E., and Maselko, J. 2013. Pelagic fish and zooplankton species assemblages in relation to water mass characteristics in the northern Bering and southeast Chukchi seas. Polar Biology, 36: 87-113.

Falk-Petersen, S., Pavlov, V., Timofeev, S., and Sargent, J. R. 2007. Climate variability and possible effects on Arctic food chains: the role of *Calanus*. *In* Arctic alpine ecosystems and people in a changing environment, pp. 147-166. Ed. by J. B. Ørbæk, R. Kallenborn, I. Tombre, E. N. Hegseth, S. Falk-Petersen and A. H. Hoel. Springer, New York. 433 pp.

Fernandes, P. G., Stevenson, P., Brierley, A. S., Armstrong, F., and Simmonds, E. J. 2003. Autonomous underwater vehicles: future platforms for fisheries acoustics. ICES Journal of Marine Science, 60: 684-691.

Fischer, J., and Visbeck, M. 1993. Seasonal variation of the daily zooplankton migration in the Greenland Sea. Deep Sea Research Part I, 40: 1547-1557.

Folt, C. L., and Burns, C. W. 1999. Biological drivers of zooplankton patchiness. Trends in Ecology and Evolution, 14: 300-305.

Geoffroy, M., Majewski, A., LeBlanc, M., Gauthier, S., Walkusz, W., Reist, J. D., and Fortier, L. 2016. Vertical segregation of age-0 and age-1+ polar cod (*Boreogadus saida*) over the annual cycle in the Canadian Beaufort Sea. Polar Biology, doi: 10.1007/s00300-015-1811-z.

George, D. 1981. Zooplankton patchiness. Report from the Freshwater Biology Association, 49: 32-44.

Greer, A. T., Cowen, R. K.,Guigand, C. M., Mcmanus, M. A., Sevadjian, J. C., and Timmerman, A. H. V. 2013. Relationships between phytoplankton thin layers and the fine-scale vertical distributions of two trophic levels of zooplankton. Journal of Plankton Research, 35: 939-956.

Harder, W. 1968. Reaction of plankton organisms to water stratification. Limnology and Oceanography, 13: 156-168.

Hobson, B. W., Bellingham, J. G., Kieft, B., McEwen, R., Godin, M. and Zhang, Y. 2012. Tethys-class long-range AUVs-extending the endurance of propeller-driven cruising AUVs from days to weeks. *In* Autonomous Underwater Vehicles (AUV), pp. 1-8. IEEE.

Houde, E. D., and Lovdal, J. D. A. 1985. Patterns of variability in ichthyoplankton occurence and abundance in Biscayne Bay, Florida. Estuarine, Coastal and Shelf Science, 20: 79-103.

Kwasniewski, S., Hop, H., Falk-Petersen, S., and Pedersen, G. 2003. Distribution of *Calanus* species in Kongsfjorden, a glacial fjord in Svalbard. Journal of Plankton Research, 25: 1-20.

La, H. S., Kang, M., Dahms, H. U., Ha, H. K., Yang, E. J., Lee, H., Kim, Y. N., et *al*. 2015. Characteristics of mesozooplankton sound-scattering layer in the Pacific Summer Water, Arctic Ocean. Deep Sea Research Part II, 120: 114-23.

Last, K. S., Hobbs, L., Berge, J., Brierley, A. S., and Cottier, F. 2016. Moonlight drives ocean-scale mass vertical migration of zooplankton during the Arctic winter. Current Biology, doi: 10.1016/j.cub.2015.11.038

Lloyd, M. 1967. Mean crowding. Journal of Animal Ecology, 36: 1-30.

Lorke, A., McGinnis, D. F., Spaak, P. and Wueest, A. 2004. Acoustic observations of zooplankton in lakes using a Doppler current profiler. Freshwater Biology, 49: 1280-1292.

Lougee, L. A., Bollens, S. M., and Avent, S.R. 2002. The effects of haloclines on the vertical distribution and migration of zooplankton. Journal of Experimental Marine Biology and Ecology, 278: 111-134.

Mackas, D. L., Kieser, R., Saunders, M., Yelland, D. R., Brown, R. M., and Moore, D. F. 1997. Aggregation of euphausiids and Pacific hake (*Merluccius productus*) along the outer continental shelf off Vancouver Island. Canadian Journal of Fisheries and Aquatic Sciences, 54: 2080-2096.

Maynou, F., Olivar, M. P., and Emelianov, M. 2006. Patchiness of eggs, larvae and juveniles of European hake *Merluccius merluccius* from the NW Mediterranean. Fisheries Oceanography, 15: 390-401.

McQuinn, I. H., Fitzgerald, G. J., and Powles, H. 1983. Environmental effects on embryos and larvae of the Isle Verte stock of Atlantic herring (*Clupea harengus harengus*). Le Naturaliste canadien, 110: 343–353.

Parker-Stetter, S. L., Rudstam, L. G., Sullivan, P. J., and Warner, D. M. 2009. Standard operating procedures for fisheries acoustic surveys in the Great Lakes, 1st edn. Great Lakes Fishery Commission, Ann Arbor. 170 pp.

Ritz, D. A. 2000. Is social aggregation in aquatic crustaceans a strategy to conserve energy? Canadian Journal of Fisheries and Aquatic Sciences, 57: 59-67.

Saloranta, T. A., and Haugan, P. M. 2001. Interannual variability in the hydrography of Atlantic water northwest of Svalbard. Journal of Geophysical Research, 106: 931-943.

Scalabrin, C., Marfia, C. and Boucher, J. 2009. How much fish is hidden in the surface and bottom acoustic blind zones? ICES Journal of Marine Science, 66: 1355-1363.

Schofield, O., Glenn, S., Orcutt, J., Arrott, M., Meisinger, M., Gangopadhyay, A., Brown, W., *et al*. 2010. Automated sensor network to advance ocean science. Eos, Transactions American Geophysical Union, 91: 345-346.

Stanton, T. K., Wiebe, P. H., Chu, D., Benfield, M. C., Scanlon, L., Martin, L., and Eastwood, R. L. 1994. On acoustic estimates of zooplankton biomass. ICES Journal of Marine Science, 51: 505-512.

Steele, E., Boyd, T., Inall, M., Dumont, E., and Griffiths, C. 2012. Cooling of the West Spitsbergen Current: AUV-based turbulence measurements west of Svalbard. *In* Autonomous Underwater Vehicles (AUV), pp. 1-7. IEEE.

Svendsen, H., Beszczynska-Møller, A., Hagen, J. O., Lefauconnier, B., Tverberg, V., Gerland, S., Ørbøk, J. B. 2002. The physical environment of Kongsfjorden–Krossfjorden, an Arctic fjord system in Svalbard. Polar Research, 21: 133-166.

Tarling, G. A., and Johnson, M. L. 2006. Satiation gives krill that sinking feeling. Current Biology, 16: 83-84.

Valle-Levinson, A., Castro, L., Cáceres, M., and Pizarro, O. 2014. Twilight vertical migrations of zooplankton in a Chilean fjord. Progress in Oceanography, 129: 114-124.

Vogedes, D., Eiane, K., Batnes, A. S., and Berge, J. 2014. Variability in *Calanus* spp. abundance on fine- to mesoscales in an Arctic fjord: implications for little auk feeding. Marine Biology Research, 10: 437-448.

Wallace, M. I., Cottier, F. R., Berge, J., Tarling, G. A., Griffiths, C., and Brierley, A. S. 2010. Comparison of zooplankton vertical migration in an ice-free and a seasonally ice-covered Arctic fjord: An insight into the influence of sea ice cover on zooplankton behaviour. Limnology and Oceanography, 55: 831-845.

Wallace, M. I., Cottier, F. R., Brierley, A. S., and Tarling, G. A. 2013. Modelling the influence of copepod behaviour on faecal pellet export at high latitudes. Polar Biology, 36: 579-592.

Tables

Table 1: Details of the AUV deployments.

Location	Date	Time (local)	Bottom depth (m)
Norskebanken	18 July 2010	06:12 – 12:35	~500
Woodfjorden	16 July 2010	13:41 – 19:11	134
Isfjordbanken	20 July 2010	20:04 – 02:04	225
Kongsfjordbanken	06 July 2010	13:44 – 17:27	~550
Kongsfjordbanken	12 July 2010	09:51 – 16:45	~550

Figure captions

Figure 1. Map of the study area indicating bathymetry and the limits of the AUV deployments (black boxes) at Norskebanken (NB), Woodfjorden (WF), Kongfjordbanken (KF), and Isfjordbanken (IF).

Figure 2. Left column: Continuous volume backscattering strength (S_v in dB re 1 m^{-1}) at (a) Norskebanken on 18 July, (b) Woodfjorden on 16 July, (c) Kongsfjordbanken on 06 July, (d) Kongsfjordbanken on 12 July, and (e) Isfjordbanken on 20 July. Local time of deployments and retrievals are indicated on the x-axis. The solid black line represents the trajectory of the AUV and the dashed black lines demarcate the SL, the IL, and the DL. Right column: Position (lat/long) and depth (colour scale) along the trajectory of each deployment.

Figure 3. Indicative profiles of (a) salinity and (b) temperature reconstructed from the five AUV deployments. The vertical resolution of the profiles is 10 metres.

Figure 4. Left column: Temperature-salinity diagrams for each deployment where the data points are the mean T-S value within a 4 m depth range corresponding to the ADCP bins. An isopycnal line (in $kg \cdot m^{-3}$) demarcating the 4 m bins with backscatter values higher (orange asterisks) and lower (black dots) than average is drawn. Right column: Vertical profiles of density gradient with a 4 m vertical resolution. The grey line is the depth of the isopycnal line in the left panel. Hatched orange lines indicate sections of the profiles with backscatter values higher than average. Note that the scale of the x-axis was one order of magnitude lower in (d) and (e).

Figure 5. Profiles of volume backscattering strength (S_v in dB re 1 m^{-1}) averaged over 4 m vertical bins. The dashed grey lines demarcate the SL, the IL, and the DL. Data from Kongsfjordbanken and Isfjordbanken are pooled in panel f, where a regression line was added for the SL and IL (dashed black line).

Figure 6. Box plots comparing the average backscatter in linear form ($m^2 \cdot m^{-3}$) for deployments around midday (Kongsfjordbanken) and midnight (Isfjordbanken) in the (a) SL, (b) IL, and (c) DL. The black line is the median, bottom and top of the rectangle are lower and upper quartiles, bottom and top whiskers are minimum and maximum values (excluding the outliers). Empty dots are outliers (more than 1.5 times the upper quartile).

Figure 7. Left column: Vertical velocity anomalies (w' in mm s^{-1}) along the trajectory of the AUV (solid black line). Right column: Corresponding profiles of w' with a resolution of 4 m (thick black lines) ± one standard deviation (grey polygons). The vertical dashed lines indicate 0 $mm \cdot s^{-1}$ and the horizontal dashed black lines demarcate the SL, the IL, and the DL.

Figure 8. Left column: Bar plots of the mean density of pelagic scatterers ($ind \cdot m^{-3}$) estimated for each layer. Right column: Corresponding bar plots of the Lloyd's patchiness index (*P*) for each layer. The dashed grey lines indicate the limit between a uniform (P <1) and a patchy distribution (P >1). Note the cut in the x-axis for Norskebanken and Woodfjorden.

Figure 9. The Lloyd's patchiness index (*P*) against the mean estimated density of pelagic scatterers ($ind \cdot m^{-3}$) for each layer of each deployment.

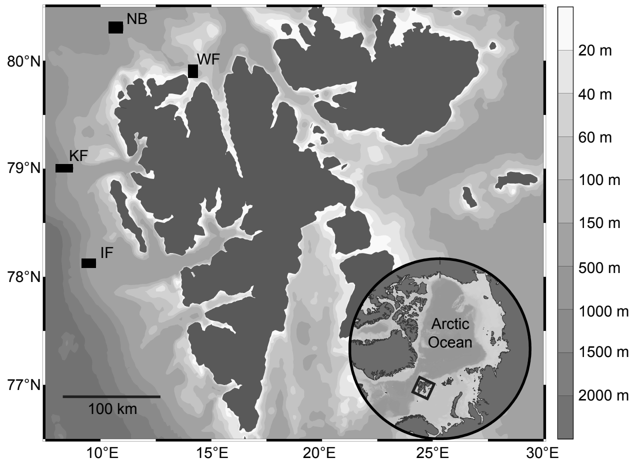

NB
WF
KF
IF
80°N
79°N
78°N
77°N
10°E
15°E
20°E
25°E
30°E
100 km
Arctic
Ocean
20 m
40 m
60 m
100 m
150 m
500 m
1000 m
1500 m
2000 m

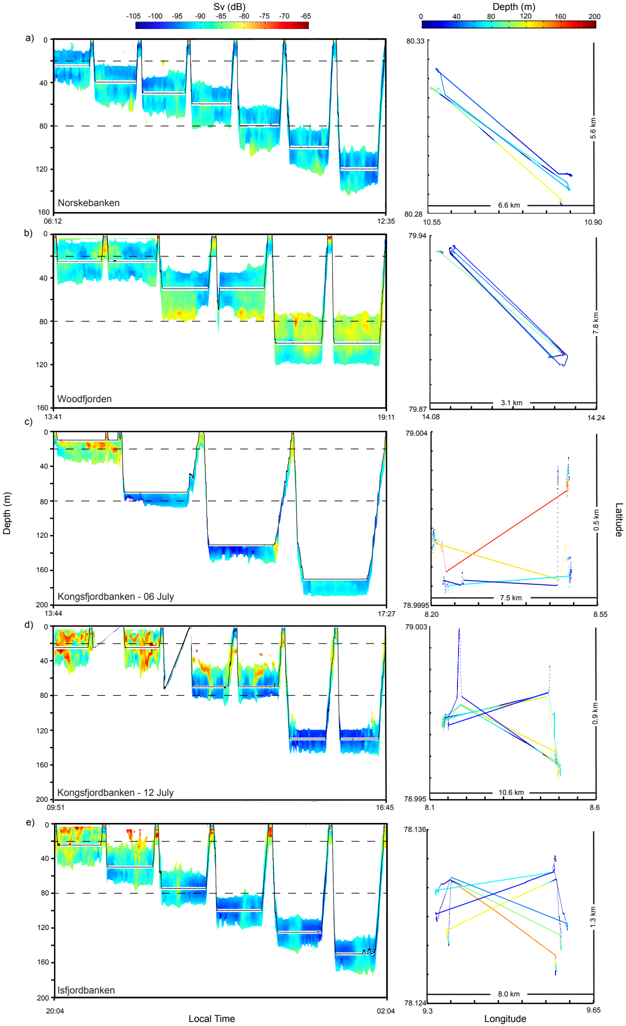

Sv (dB)
-105 -100 -95 -90 -85 -80 -75 -70 -65
Depth (m)
0 40 80 120 160 200
a)
Norskebanken
06:12
12:35
80.33
80.28
10.55
10.90
6.6 km
5.6 km
b)
Woodfjorden
13:41
19:11
79.94
79.87
14.08
14.24
3.1 km
7.8 km
c)
Kongsfjordbanken - 06 July
13:44
17:27
79.004
78.9995
8.20
8.55
7.5 km
0.5 km
d)
Kongsfjordbanken - 12 July
09:51
16:45
79.003
78.995
8.1
8.6
10.6 km
0.9 km
e)
Isfjordbanken
20:04
02:04
78.136
78.124
9.3
9.65
8.0 km
1.3 km
Depth (m)
Local Time
Longitude
Latitude

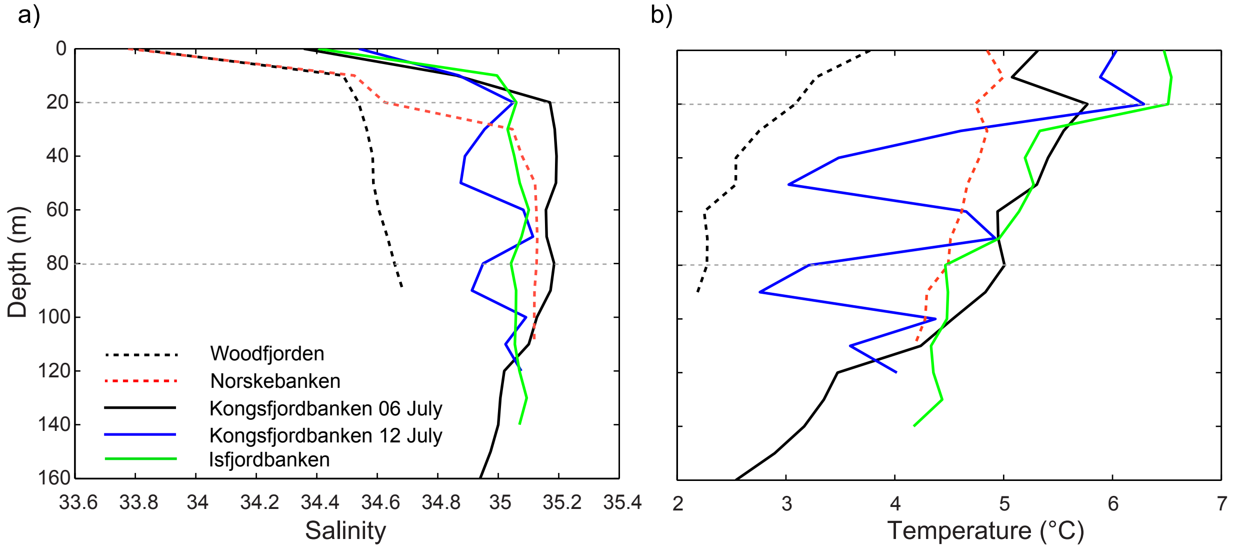

a)
b)
Depth (m)
0
20
40
60
80
100
120
140
160
33.6
33.8
34
34.2
34.4
34.6
34.8
35
35.2
35.4
Salinity
Woodfjorden
Norskebanken
Kongsfjordbanken 06 July
Kongsfjordbanken 12 July
Isfjordbanken
2
3
4
5
6
7
Temperature (°C)

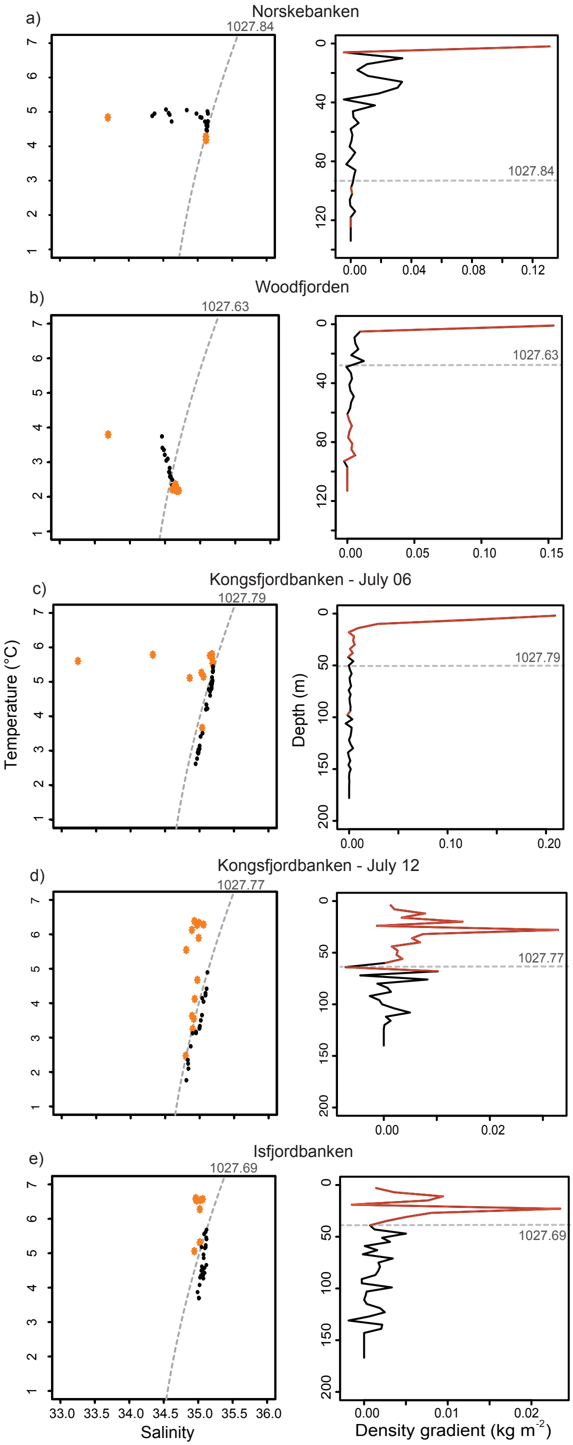
a)
Norskebanken
1027.84
b)
Woodfjorden
1027.63
c)
Kongsfjordbanken - July 06
1027.79
d)
Kongsfjordbanken - July 12
1027.77
e)
Isfjordbanken
1027.69
Temperature (°C)
Depth (m)
Salinity
Density gradient (kg m-2)

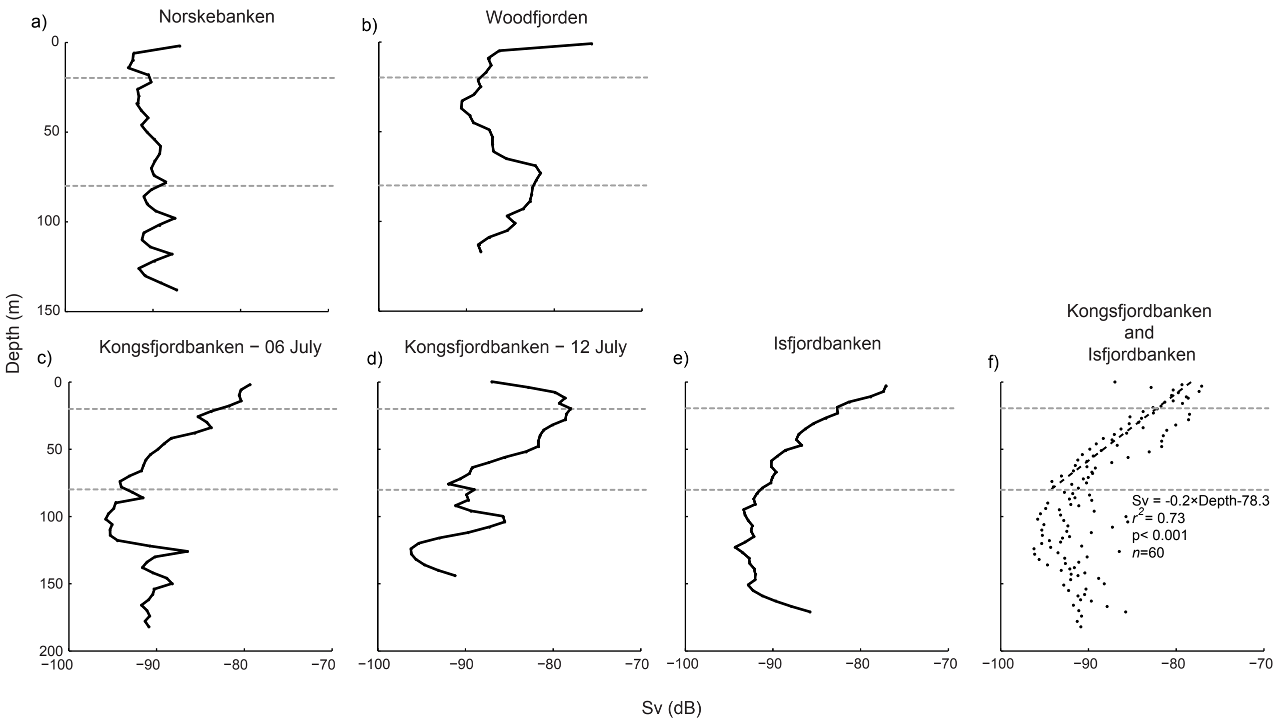

a)
Norskebanken
b)
Woodfjorden
c)
Kongsfjordbanken − 06 July
d)
Kongsfjordbanken − 12 July
e)
Isfjordbanken
f)
Kongsfjordbanken and Isfjordbanken
Sv = -0.2×Depth-78.3
r^2 = 0.73
p< 0.001
n=60
Depth (m)
Sv (dB)
0
50
100
150
200
−100
−90
−80
−70

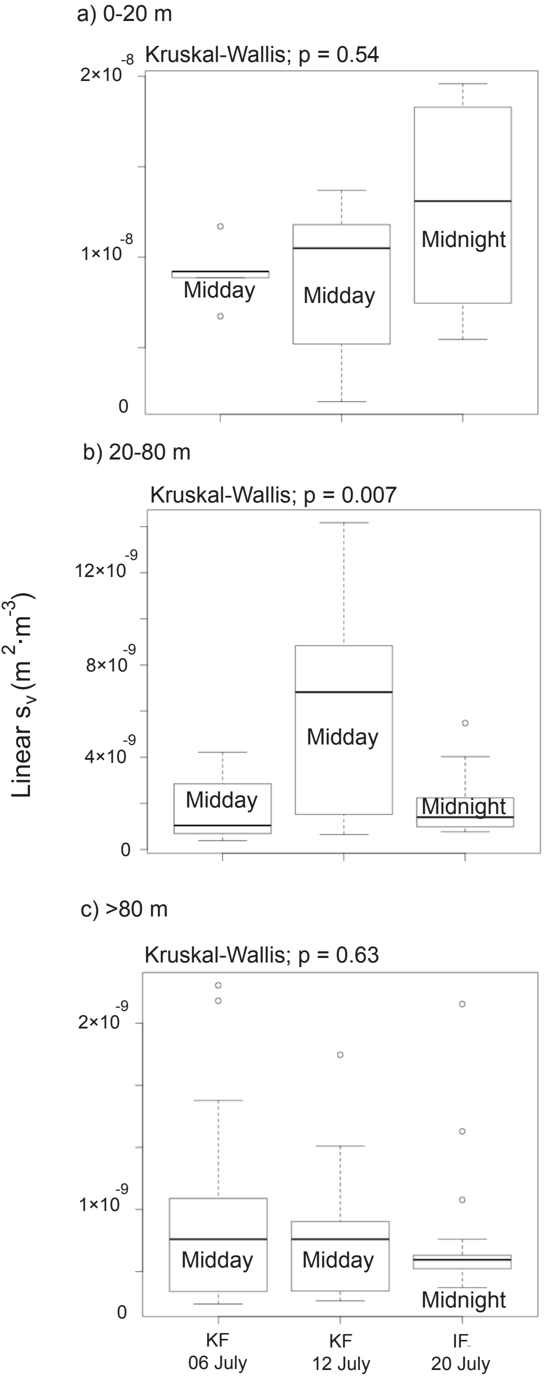
a) 0-20 m
Kruskal-Wallis; p = 0.54
2×10^{-8}
1×10^{-8}
0
Midday
Midday
Midnight
b) 20-80 m
Kruskal-Wallis; p = 0.007
12×10^{-9}
8×10^{-9}
4×10^{-9}
0
Midday
Midday
Midnight
c) >80 m
Kruskal-Wallis; p = 0.63
2×10^{-9}
1×10^{-9}
0
Midday
Midday
Midnight
Linear s_V ($m^2 \cdot m^{-3}$)
KF
06 July
KF
12 July
IF
20 July

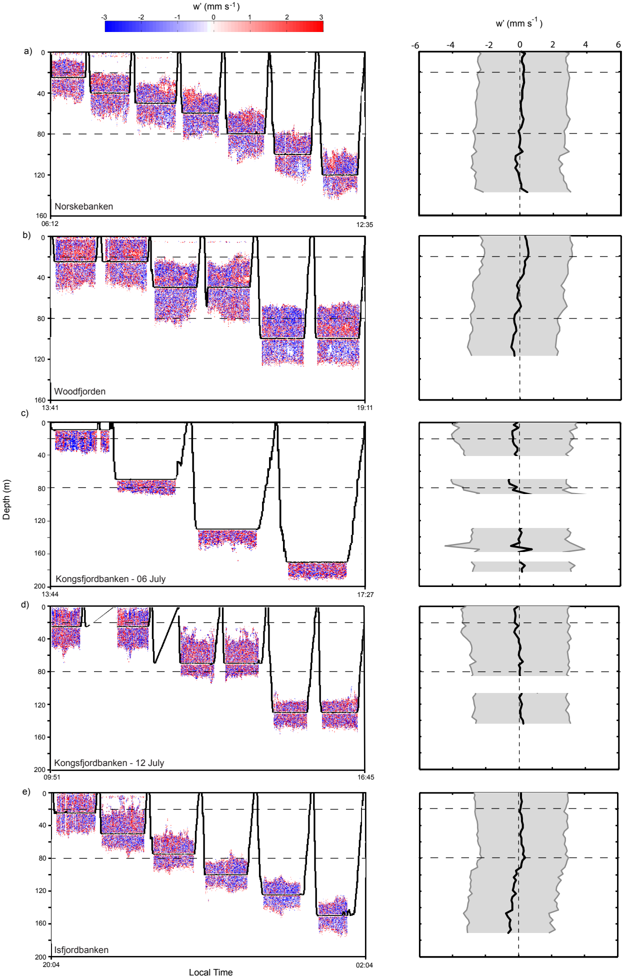

w' (mm s-1)
-3
-2
-1
0
1
2
3
w' (mm s-1)
-6
-4
-2
0
2
4
6
a)
b)
c)
d)
e)
Depth (m)
Norskebanken
06:12
12:35
Woodfjorden
13:41
19:11
Kongsfjordbanken - 06 July
13:44
17:27
Kongsfjordbanken - 12 July
09:51
16:45
Isfjordbanken
20:04
02:04
Local Time

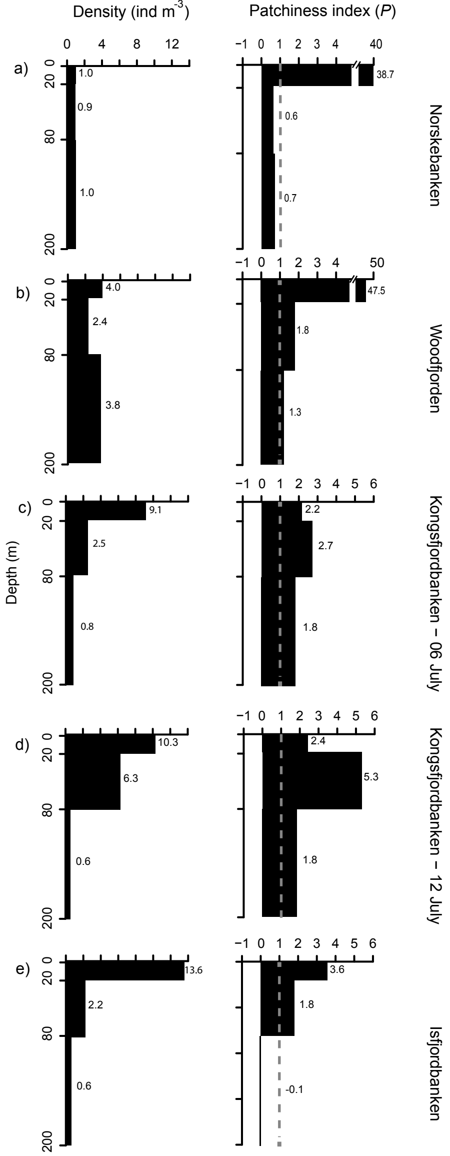

Density (ind m-3)
Patchiness index (P)
0 4 8 12
−1 0 1 2 3 4 40
a)
0
20
80
200
1.0
0.9
1.0
38.7
0.6
0.7
Norskebanken
−1 0 1 2 3 4 50
b)
4.0
2.4
3.8
47.5
1.8
1.3
Woodfjorden
−1 0 1 2 3 4 5 6
c)
9.1
2.5
0.8
2.2
2.7
1.8
Kongsfjordbanken – 06 July
Depth (m)
d)
10.3
6.3
0.6
2.4
5.3
1.8
Kongsfjordbanken – 12 July
e)
13.6
2.2
0.6
3.6
1.8
-0.1
Isfjordbanken

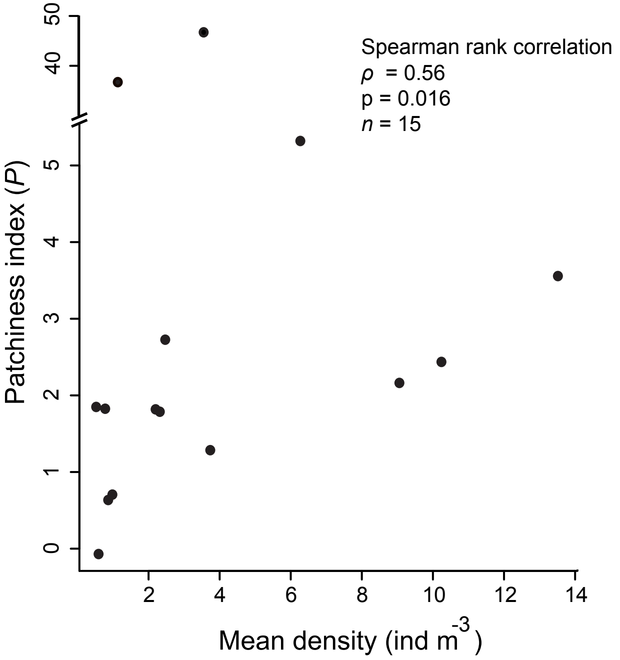
Spearman rank correlation
ρ = 0.56
p = 0.016
n = 15
Patchiness index (P)
Mean density (ind m-3)
0
1
2
3
4
5
40
50
2
4
6
8
10
12
14